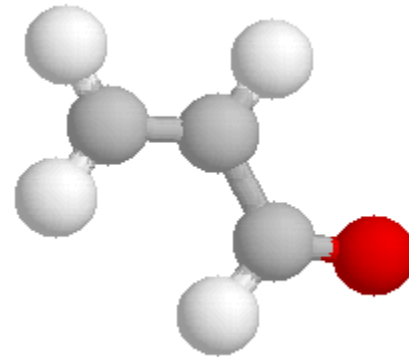


10 μm High-Resolution Spectra of Acrolein (*trans*-form)

assignments for ν_{14} and ν_{16} bands



**Objective - to provide benchmark high-resolution laboratory
data in the 10 μm region for smoke detection**

X.J. Jiang, J.M. Fisher, Li-Hong Xu

Centre for Laser, Atomic and Molecular Sciences (CLAMS),
Dept of Physical Sciences, Univ. of New Brunswick, Saint John, NB, Canada

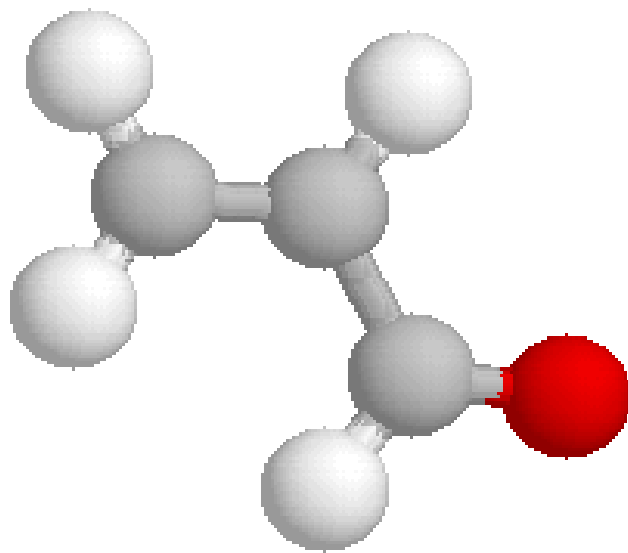
A.R.W. McKellar

Steacie Institute for Molecular Sciences, National Research Council of Canada,
Ottawa, Canada

Acrolein

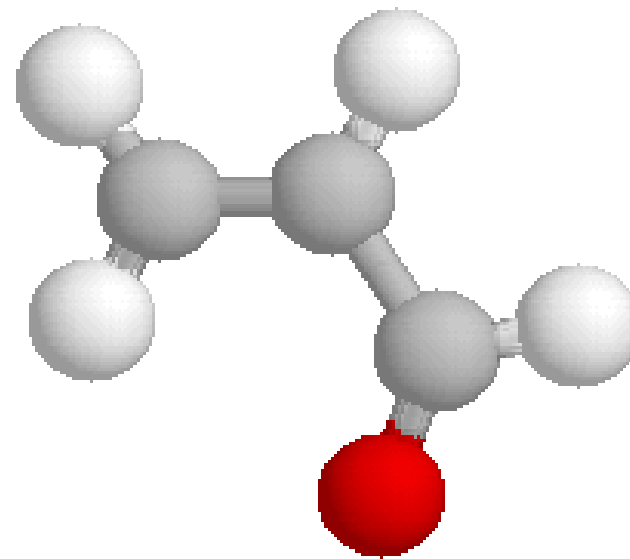


C_s symmetry



trans-form

$$E_{\text{elec.}} = -191.9742621 \text{ (Hartree)}$$



cis-form

$$E_{\text{elec.}} = -191.9707933 \text{ (Hartree)}$$

$$\Delta E_{\text{elec.}} \sim 760 \text{ cm}^{-1}$$

$$1 \text{ Hartree} = 219474 \text{ cm}^{-1}$$

Based on *ab initio* calculation at B3LYP/6-311++G** using Gaussian03

Introduction - environmental and health concerns

- Acrolein plays an important role in pollution and is listed in **US-EPA 188 Hazardous Air Pollutants (HAPs)**
- It is one of the priority mobile air toxics
(Acetaldehyde, Acrolein, Benzene, 1,3-Butadiene, Formaldehyde, Diesel Particulate Matter + Diesel Exhaust Organic Gas)
Source: J. Wilson, FHWA Air Toxics Workshop, Chicago, IL, May 12, 2003
- It is principally used as a chemical intermediate in the production of acrylic acid and its esters
- Combustion of fossil fuels and tobacco smoke contribute to the environmental prevalence of acrolein

Hazardous Air Pollutants (HAP) Detection Methods

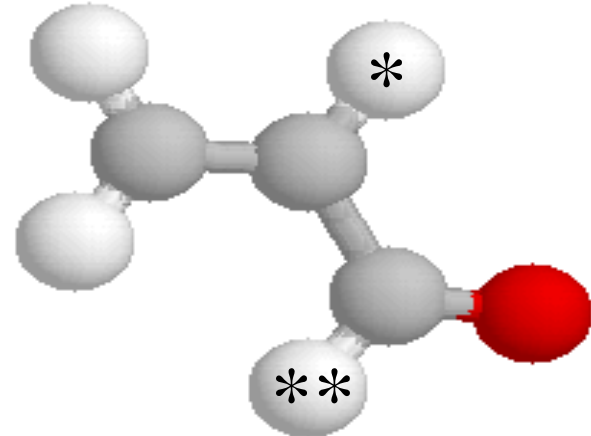
- GC-MS
 - MS-MS
 - Proton Transfer MS
 - FTIR (low resolution IR)
 - Open path atmospheric P
 - **Tunable Infrared Laser Differential Absorption Spectroscopy (TILDAS)**
 - Extractive sampling, low P
 - Continuous
 - High Speed < 1 s
 - High Resolution
 - High Sensitivity
 - Absolute Concentrations
- Sub-List of HAPs Most Applicable to TILDAS Detection Methods
- Acetaldehyde *
 - Acrolein *
 - Acrylonitrile
 - 1-3 Butadiene *
 - Benzene
 - Carbonyl Sulfide
 - Ethylene Oxide
 - Formaldehyde
 - Formic Acid
 - Hydrazine
 - Methanol *
- * currently targeted molecules

Philip Morris Research Center, Inc. & Aerodyne Research, Inc. & VA.

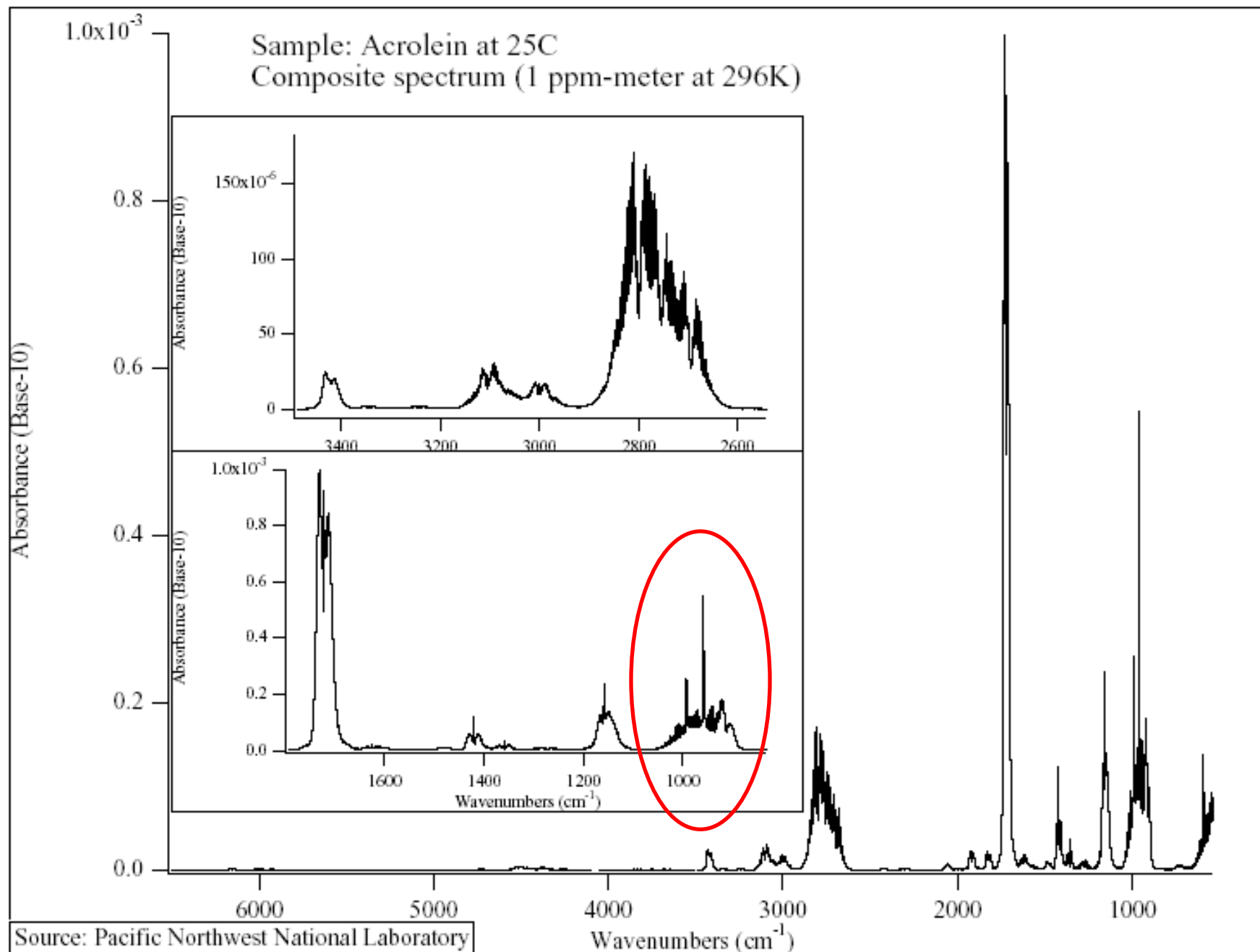
High resolution data are needed, and are not yet available in literature

Vibrational modes of acrolein (*trans*-form)

A'	Description	Obs (cm ⁻¹)	Vib. degrees of freedom: $3x8 - 3T - 3R = 18$		
v ₁	=CH ₂ a-str	3103			
v ₂	CH* str	3069			
v ₃	=CH ₂ s-str	2998			
v ₄	CH** str	2800			
v ₅	C=O str	1742			
v ₆	C=C str	1625			
v ₇	=CH ₂ sci	1420			
v ₈	CH** bend	1360	A''	Description	Obs (cm ⁻¹)
v ₉	CH* bend	1275	v ₁₄	=CH ₂ twist	993
v ₁₀	C-C str	1158	v ₁₅	CH** o/p	972
v ₁₁	=CH ₂ i/p	912	v ₁₆	=CH ₂ o/p	959
v ₁₂	CCO bend	564	v ₁₇	CH* o/p	593
v ₁₃	CCC bend	324	v ₁₈	C-C tor	158



Survey spectrum of Acrolein - Pacific Northwest National Laboratory



Acrolein (*trans*-form): High Resolution Spectroscopy

- Low energy ***trans*-form** has been studied extensively by microwave spectroscopy;
- No previous high-resolution studies exist for the 10 μm region;
- High-resolution FTIR spectra have been recorded at the National Research Council of Canada from 800 – 1100 cm^{-1} @ 0.002 cm^{-1} resolution at room and cooled temp.

Spectrum I: 295K, 30 cm multi-pass cell set to 4 transits, ~500 mTorr

Spectrum II: 180K, 2 m multi-pass cell set to 4 transits, ~60 mTorr

cover at least the ν_{11} (A' CH_2 rocking, in-plane), 912 cm^{-1}

ν_{16} (A" CH_2 wagging, out-of-plane) 959 cm^{-1}

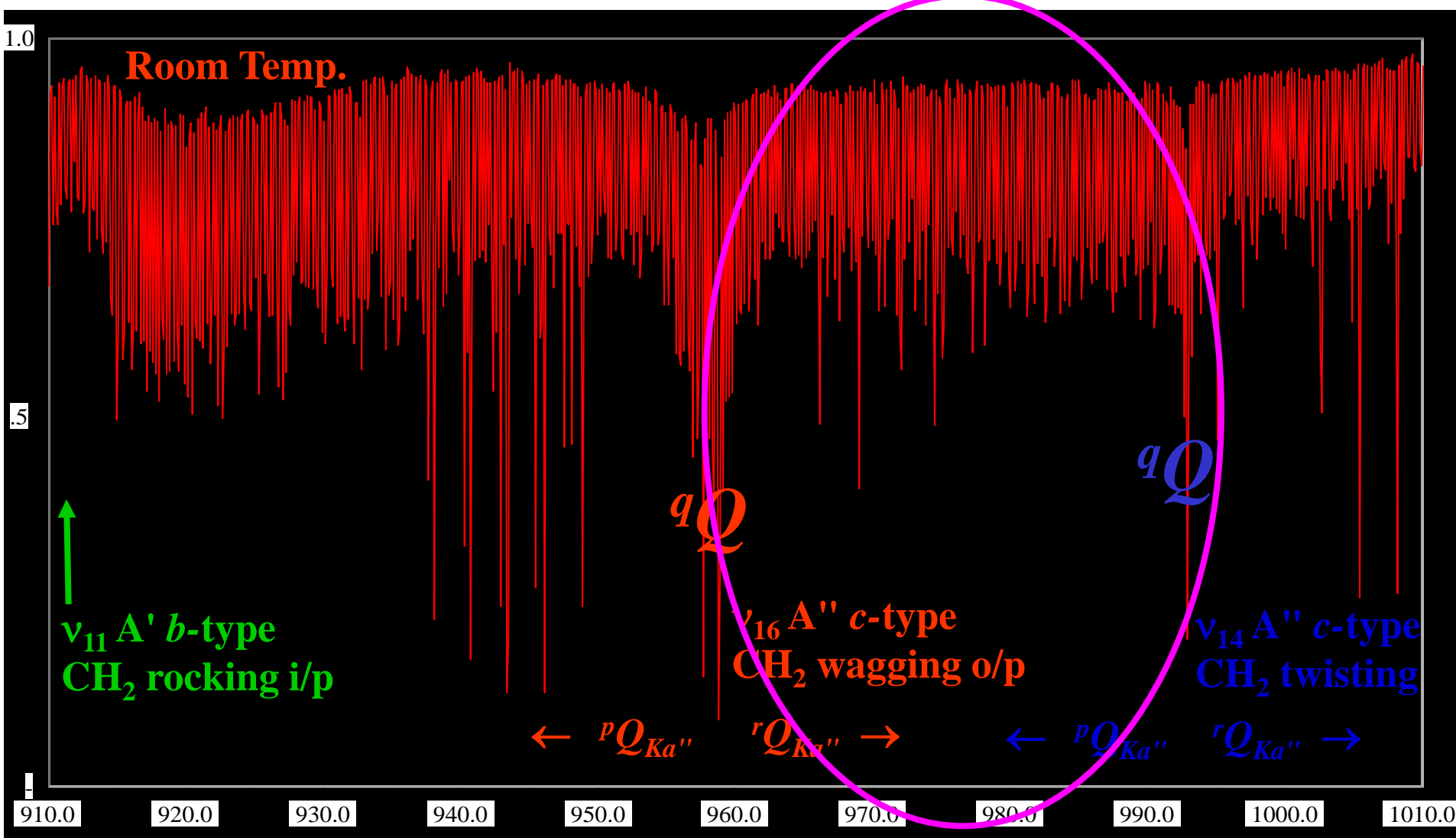
ν_{14} (A" CH_2 twisting) 993 cm^{-1}

- Rotational analyses of the

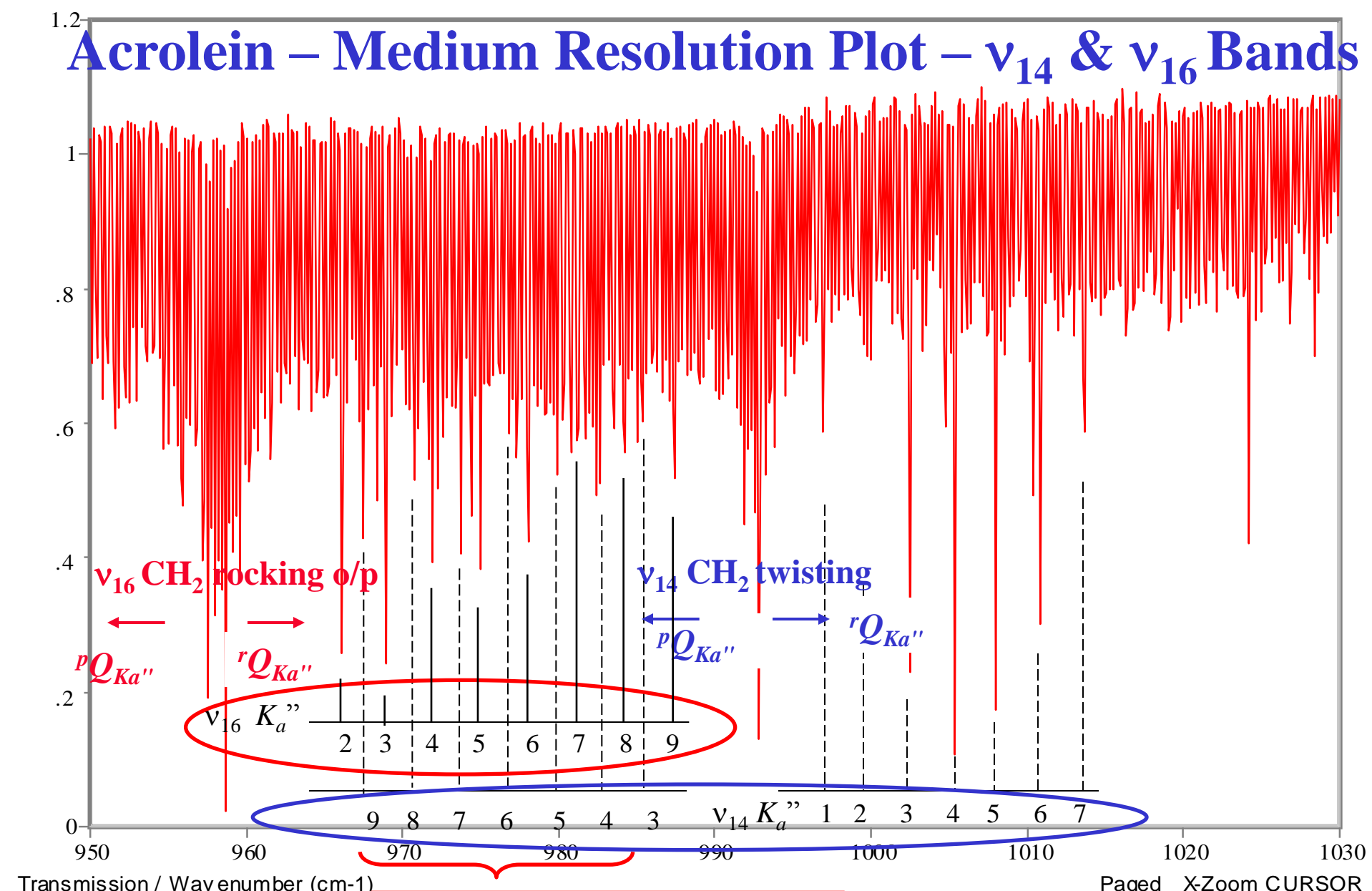
ν_{16} and ν_{14} bands – both c-types

are reported here.

Acrolein – Low Resolution Plot – ν_{11} , ν_{16} , ν_{14} modes



Acrolein – Medium Resolution Plot – ν_{14} & ν_{16} Bands



Transmission / Wavenumber (cm⁻¹)

Paged X-Zoom CURSOR

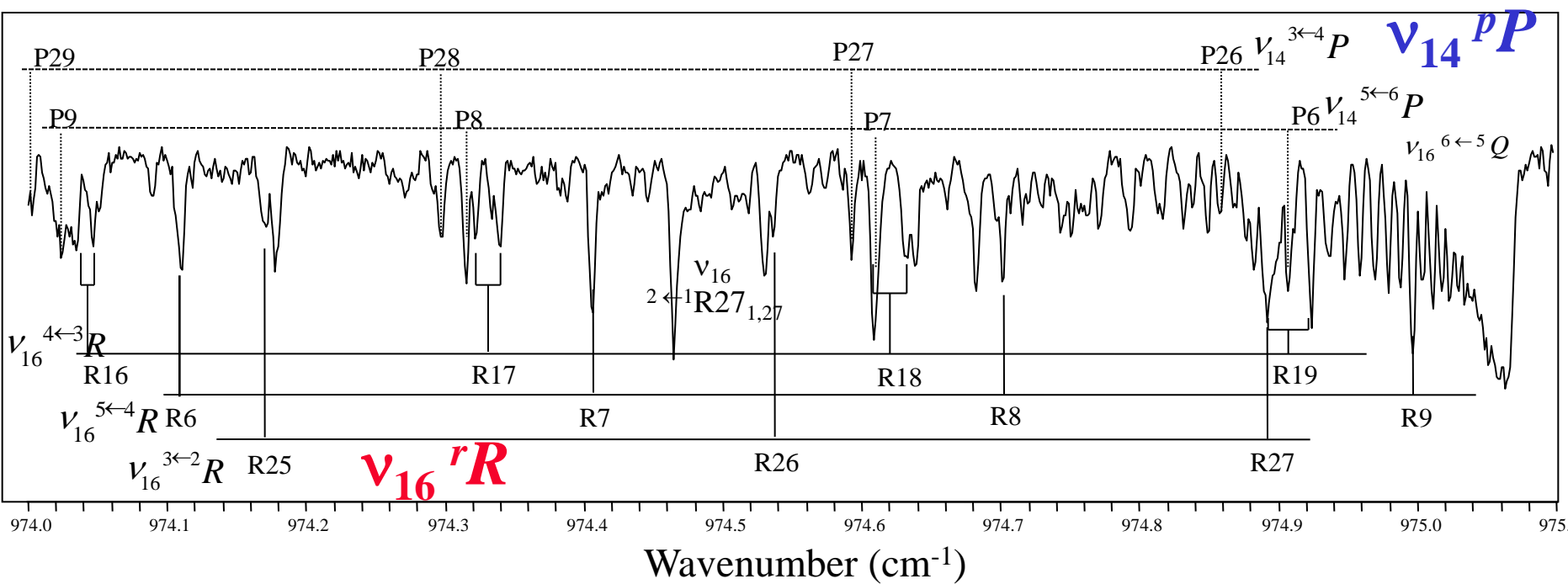
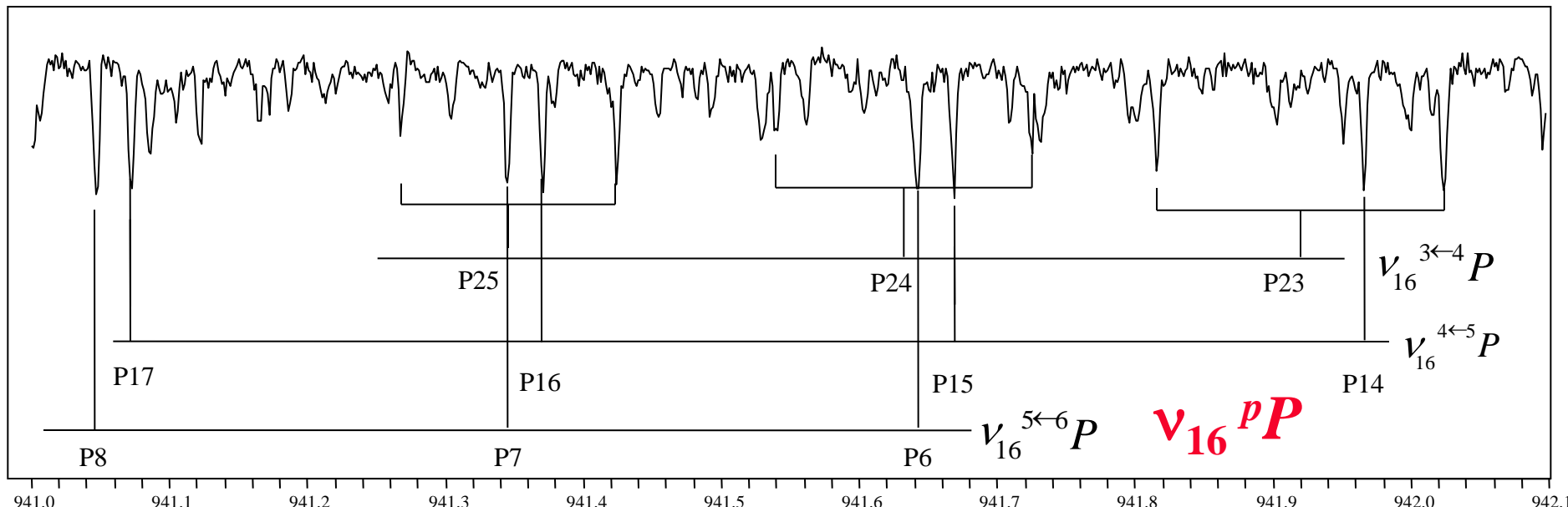
File # 1 = AP2804~1

4/28/2004 4:59 PM Res=.0021

2m cell , 4pass, 0.06 Torr acrolein

rQ of ν_{16} and pQ of ν_{14} overlap to some extent

High Resolution Display



Modeling – Watson Asymmetric Rotor Hamiltonian (isolated band approach)

- **ν_{18} (ground state):**
 - 270 MW transitions were previously measured in the literature.
 - They were refitted for refined ground state parameters.
- **ν_{16} (A'' CH₂ out-of-plane wagging):**
 - Upper states have been identified for $K_a' = 0$ to 10.
 - Small asymmetry splittings for $K_a' < 5$ have been observed.
 - The band has been modeled by a Watson asymmetric rotor Hamiltonian with $K_a' = 7$ and 8 excluded.
- **ν_{14} (A'' CH₂ twisting):**
 - Upper states have been identified for $K_a' = 1$ to 9.
 - Small asymmetry splittings for $K_a' < 5$ have been observed.
 - The band has been modeled by a Watson asymmetric rotor Hamiltonian with $K_a' = 1-3$ excluded.

Molecular Parameters

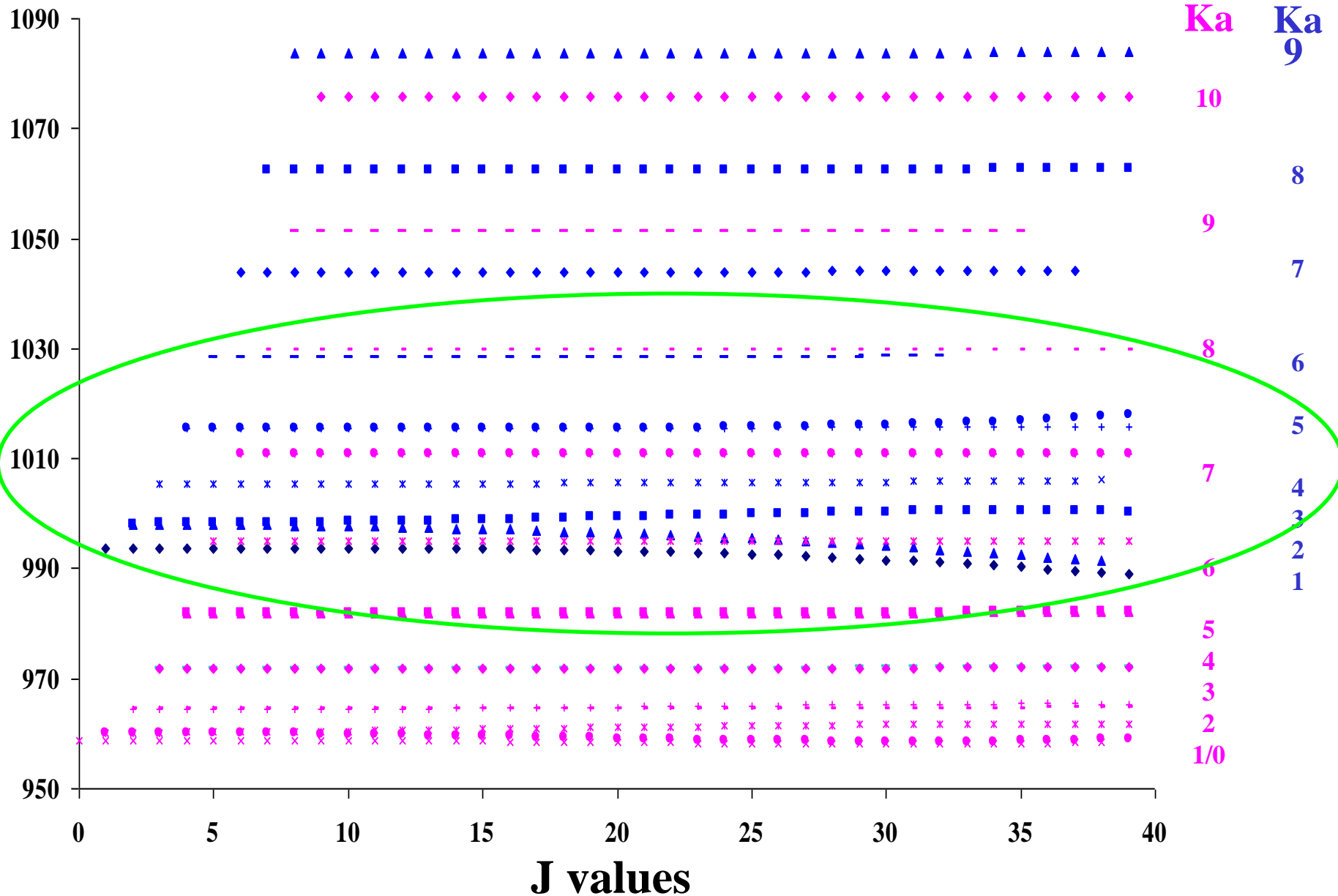
	Ground State^a	ν_{16} (CH_2 wagging)	ν_{14} (CH_2 twisting)
ν_{vib}	0.0	958.74075(11)	992.65739(69)
A	1.57954994(15)	1.596714(10)	1.570188(54)
B	0.1554241692(67)	0.15529624(80)	0.155220(16)
C	0.1415208986(73)	0.14152245(82)	0.141938(19)
$\Delta_K \times 10^5$	1.2023(16)	2.506(26)	0.76(13)
$\Delta_{JK} \times 10^6$	-0.292890(96)	-0.286(13)	1.058(63)
$\Delta_J \times 10^7$	0.34750(12)	0.3543(31)	
$\delta_J \times 10^8$	0.39988(35)	0.458(30)	
$\delta_K \times 10^5$	0.0193(89)	0.1026(76)	-1.000(19)
$H_K \times 10^7$		-0.137(19)	-0.385(95)
$H_{KJ} \times 10^8$	-0.001594(34)	-0.571(10)	1.688(50)
$H_{JK} \times 10^{10}$	-0.0029(18)	-0.146(69)	
# of lines	270	962 ($K_a = 7, 8$ excluded)	552 ($K_a = 1-3$ excluded)
RMS	0.017 MHz	0.0010 cm ⁻¹	0.0013 cm ⁻¹

^a Ground state parameters have been converted to cm⁻¹ for ready comparison.

(cm⁻¹)

J-Reduced Energy Diagram

v_{16} v_{14}
Ka Ka
9 9



Summary and Future

- To a large extent, the ν_{16} (A'') **c-type CH₂ out-of-plane wagging band** (959 cm⁻¹) and ν_{14} (A'') **c-type CH₂ twisting band** (993 cm⁻¹) can be modeled by a Watson asymmetric rotor Hamiltonian, treating each state separately with some subbands excluded (we believe states excluded are perturbed);
- We plan to carry out analysis for the ν_{11} (A') **CH₂ in-plane rocking mode** (912 cm⁻¹) next, as state interactions are expected between ν_{11} , ν_{16} and ν_{14} . Indeed, we have observed some irregular *J* and *K* patterns in ν_{16} and ν_{14} . In order to treat the spectra properly, it might be helpful to use an interacting band model;
- We have just started to model the ν_{14} and ν_{16} states simultaneously with inclusion of symmetry allowed terms between the ν_{14} and ν_{16} .
- In future, further low temp FTIR spectra would be really helpful with the new Bruker IFS125 HR FTS (0.0009 cm⁻¹ unapodized max. res.) at the **Canadian Light Source** in Saskatoon.

Acknowledgements: financial support from NSERC; thanks to Dr. M.S. Zahniser at Aerodyne Research, Inc., for bringing up this interesting subject of study.

Line Intensity Calculation

$$S_{ij} = \varepsilon \frac{8\pi^3}{3hc} v_{ij} \otimes \frac{T_o}{TZ_v Z_t Z_r} [1 - e^{-\frac{hc\nu_{ij}}{kT}}] e^{-\frac{hcE_i}{kT}}$$

$$|\langle \mu \rangle|^2 A \langle J' K' \leftarrow J'' K'' \rangle$$

- ε: Nuclear spin statistical weight
 ν_{ij}: Transition frequency
 ⊗: Loschmidt's number
 T: Temperature
 Z: Partition functions (vib, tors, rot)
 |⟨μ⟩|^2: Transition moment - vibrational
 A: Honl-London factor – rot. overlap

Ab initio Dipole Derivative Calculation

➤ Structure & frequency calculation with Gaussian 03 at B3LYP/6-311++G**

- Eigenvectors (displacements) for each normal mode

(standard orientation, normalized, not orthogonal):
 multiplied by (m_{rd_n})^{1/2} ⇒ PAM

$$\left\{ \frac{dx}{dQ_n}, \frac{dy}{dQ_n}, \frac{dz}{dQ_n} \right\}_{i=1 \text{ to } N} \quad (n = 1 \text{ to } 3N-6)$$

- Dipole derivative

(in z-matrix orientation) ⇒ PAM

$$\left\{ \frac{d\mu_g}{dx}, \frac{d\mu_g}{dy}, \frac{d\mu_g}{dz} \right\}_{i=1 \text{ to } N} \quad (g = x, y, z)$$

- Dipole derivatives

for each normal mode
 in PAM system

$$\frac{d\mu_g}{dQ_n} = \left\{ \left\{ \frac{d\mu_g}{dx}, \frac{d\mu_g}{dy}, \frac{d\mu_g}{dz} \right\}_i \right\} \bullet \left\{ \left\{ \frac{dx}{dQ_n}, \frac{dy}{dQ_n}, \frac{dz}{dQ_n} \right\}_i \right\}$$

Vibrational modes of acrolein (*trans*-form)

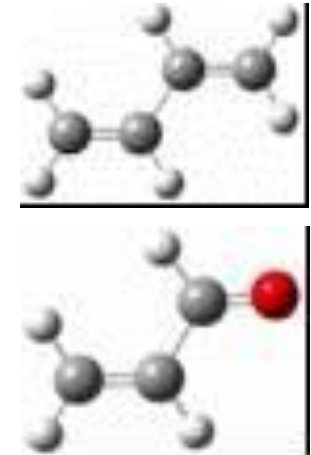
A'	Description	Obs (cm ⁻¹)	A''	Description	Obs (cm ⁻¹)
v ₁	=CH ₂ a-str	3103			
v ₂	CH* str	3069			
v ₃	=CH ₂ s-str	2998			
v ₄	CH** str	2800			
v ₅	C=O str	1742			
v ₆	C=C str	1625			
v ₇	=CH ₂ sci	1420			
v ₈	CH** bend	1360			
v ₉	CH* bend	1275	v ₁₄	=CH ₂ twist	993
v ₁₀	C-C str	1158	v ₁₅	CH** o/p	972
v ₁₁	=CH ₂ i/p	912	v ₁₆	=CH ₂ o/p	959
v ₁₂	CCO bend	564	v ₁₇	CH* o/p	593
v ₁₃	CCC bend	324	v ₁₈	C-C tor	158

High-resolution FTIR spectra have also been recorded at NRC in FIR region

Convering:

Low frequency vibrations and v₁₈ hot band
Analysis is in progress - A.R.W. McKellar
NRC

10 μm High-Resolution Spectra of 1,3-Butadiene $\text{H}_2\text{C}=\text{C(H)-C(H)=CH}_2$ ($\text{C}_{2\text{h}}$)



Acrolein

$\text{H}_2\text{C}=\text{C(H)-C(H)=O}$ (C_s)

**Objective - to provide and extend benchmark high-resolution
laboratory data for the two molecules in the 10 μm region**

Li-Hong Xu, X.J. Jiang, J. Fisher, Z.D. Sun, R.M. Lees

Centre for Laser, Atomic and Molecular Sciences (CLAMS),
Dept of Physical Sciences, Univ. of New Brunswick, Saint John, NB, Canada

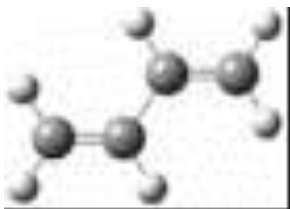
N.C. Craig

Dept. of Chemistry,
Oberlin College,
Ohio, U.S.A.

A.R.W. McKellar

Steacie Institute for Molecular Sciences,
National Research Council of Canada,
Ottawa, Canada

1,3-Butadiene $\text{H}_2\text{C}=\text{C(H)-C(H)=CH}_2$



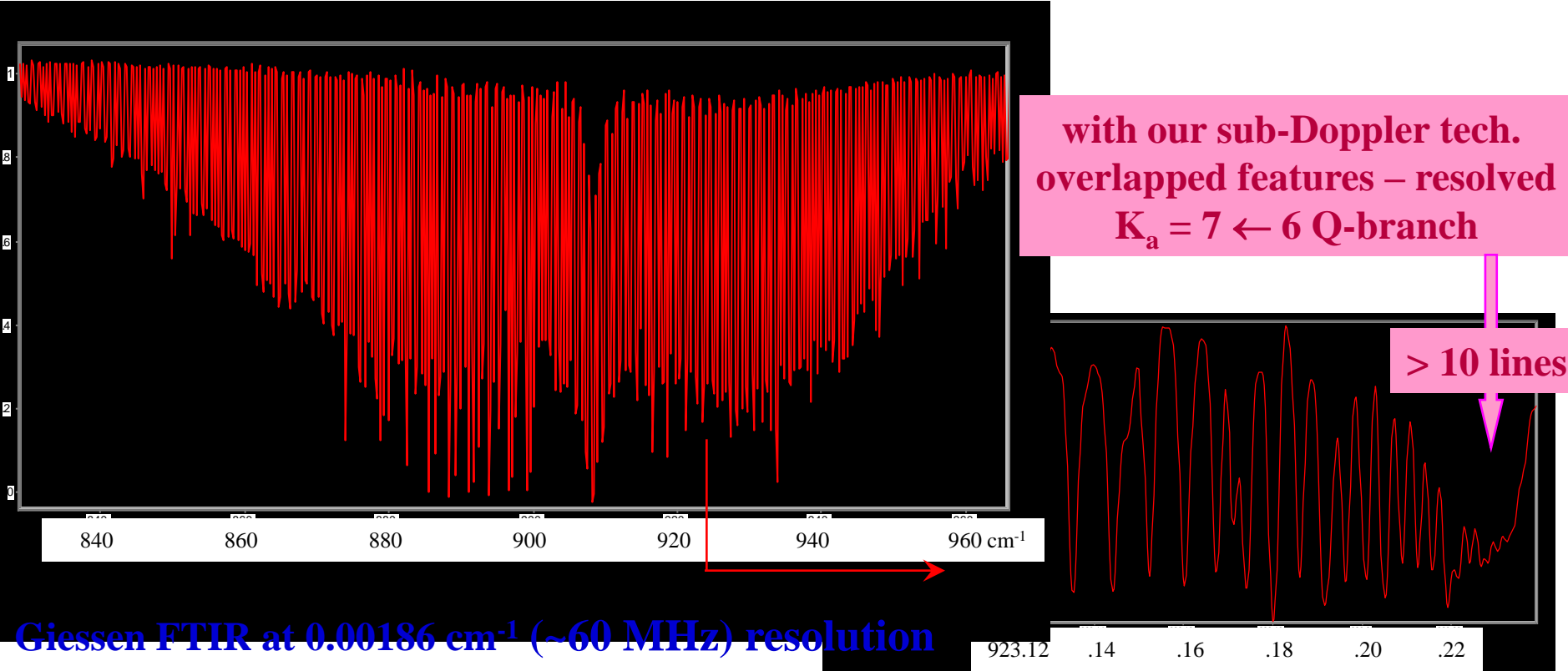
$\text{C}_{2\text{h}}$ symmetry

- Lower energy planar *trans*-form belongs to the $\text{C}_{2\text{h}}$ symmetry group.
- Normal isotopic species is non-polar, prohibiting traditional MW spectroscopy.
- **1,3-Butadiene, ν_{11} (a_u) CH_2 wagging mode - centred in 11 μm region**
 - FTIR spectrum has been recorded in Giessen at 0.00186 cm^{-1} ($\sim 60 \text{ MHz}$) resolution and rotationally analyzed by N.C. Craig *et al.*, J. Mol. Struct. **695-696** (2004) 59-69.
 - Many medium and low J Q -branch component lines are not resolved in the Doppler limited Fourier transform spectra.
 - We have applied the **saturation Lamb-dip technique** ($\sim 200 \text{ kHz}$) to the present case (using **CO₂/MWSB**). Several ' Q '-branches have been completely resolved.
 - For intensity information, a line list with position and intensity has been compiled using ***ab initio* dipole derivative** & rotational constants from high resol'n analysis, Z.D. Sun *et al.*, J. Mol. Struct. **742** (2005) 69-76.

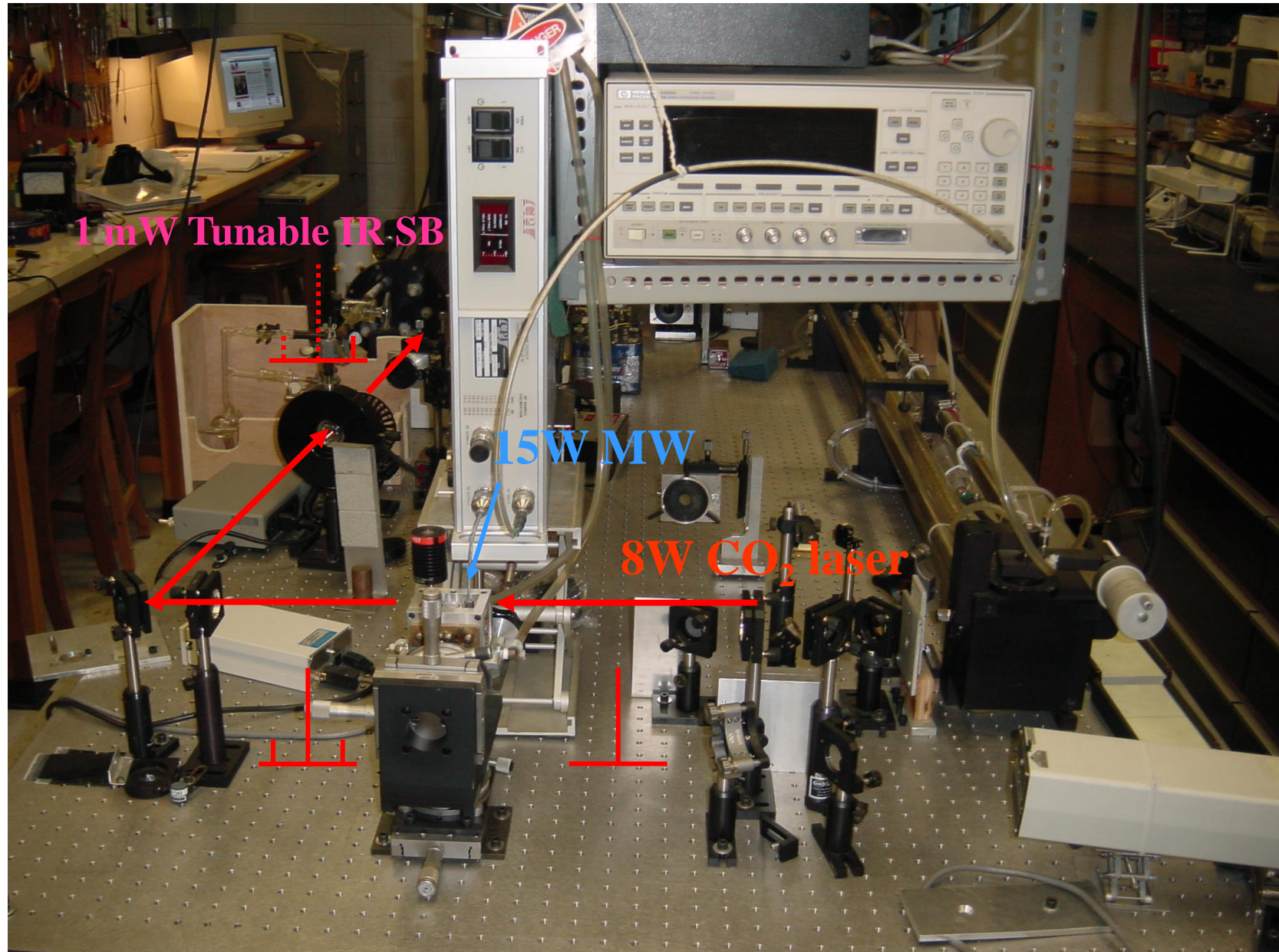
1,3-Butadiene



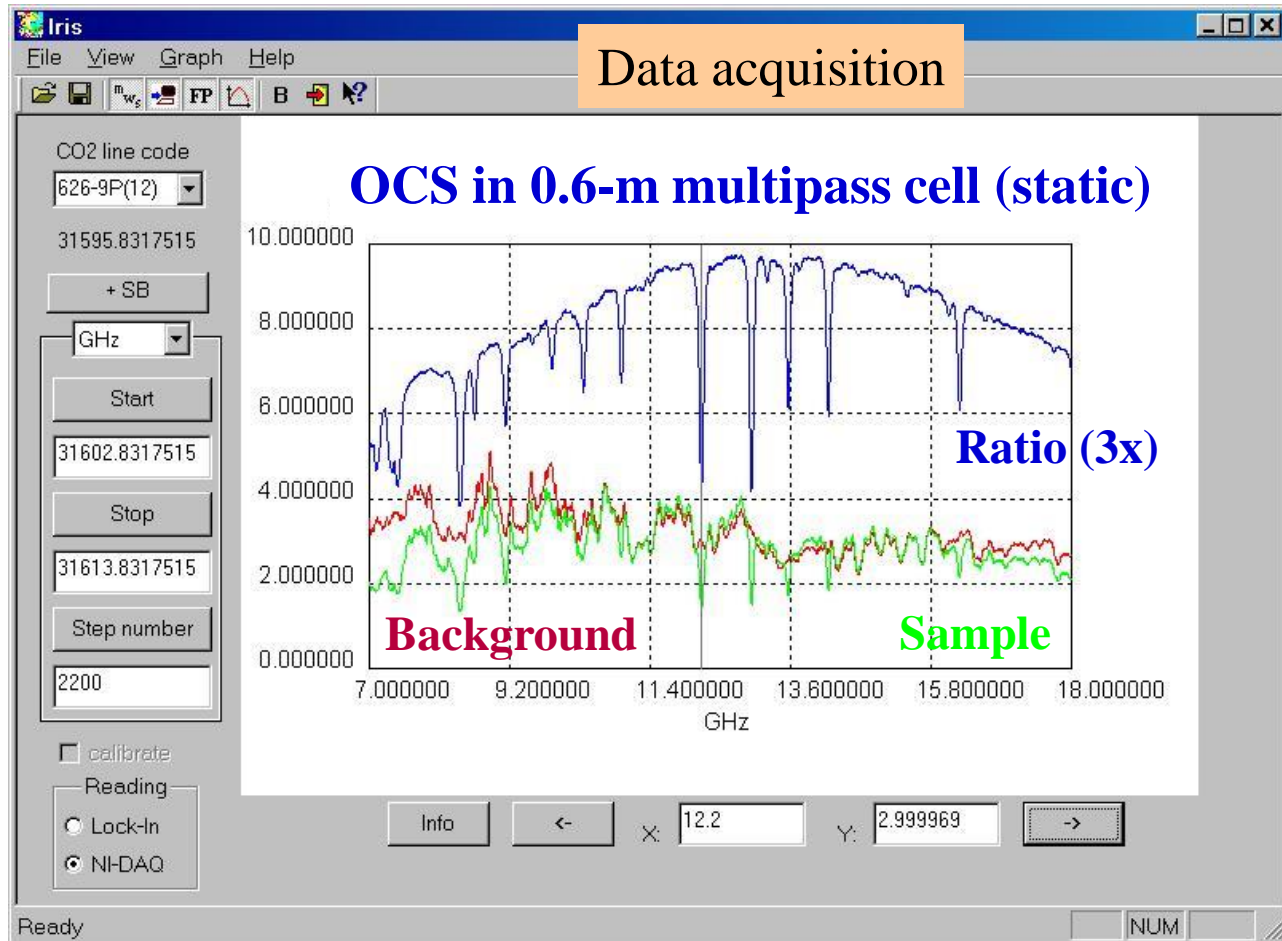
- used in the production of rubber and plastics.
- detected in ambient air (released from motor vehicle exhaust) - 0.3 ppb.
- expected in the cigarette smoke matrix (1 of the 4 target molecules in 2004).
- at Aerodyne Research Inc. & Philip Morris Research Center, quantum cascade laser system is commissioned – **reliance on lab benchmark database**.



Optical Table Layout



Frequency Sweeping, PZT Tuning & Data Acquisition



Saturation Lamb-dip experiments
@ sub-Doppler resolution (~ 200 kHz)

Methanol (CH₃OH), OCS, Butadiene (C₄H₆)
in collaboration with colleagues in NNOV-Russia

MW frequency sweeping

GHz

Low

7

High

18

Step size

0.005

Low start

Test

High start

Two way

Continuously

on step confirmation

Control

Connect

Set start

Start scan

Step UP

Step DOWN

Delay (ms): 500

Max power: 3 dBm

Power curve: TOP

F-P PZT voltage tuning

Set voltage (0-999V): 712

Volt step size: 0.5

Scan to voltage (0-999V): 999

Change voltage each ... GHz: 0.3

Enable change after ... GHz

Change at ... V: 5

Change to ... %: 96

Search step limit: 500

Change NOW

Set

<- >

Scan

Connect

Change NOW

Search step limit

Report

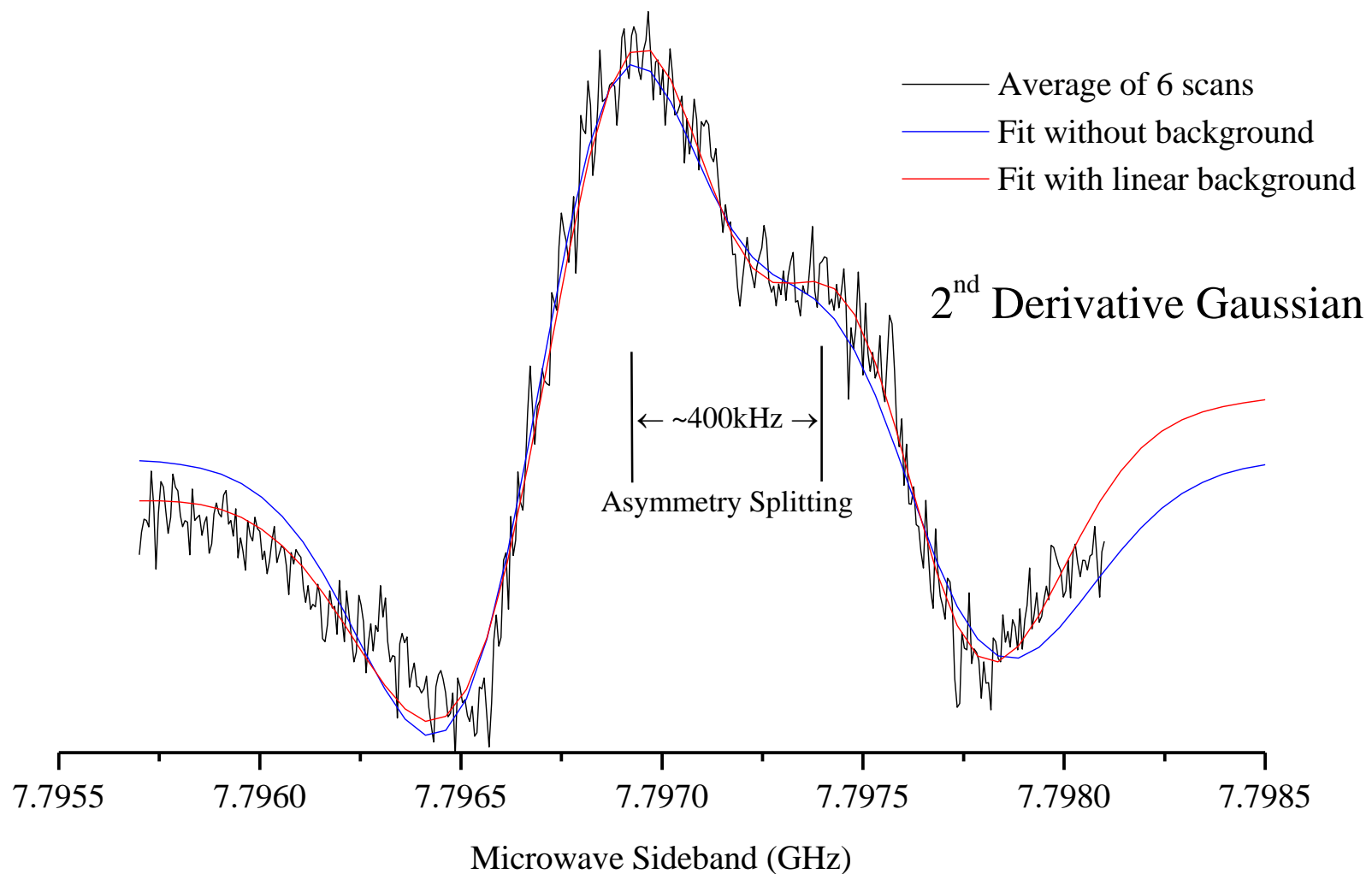
Calibrate

One-Off

After change voltage delay (ms): 500

10P42 CO₂ Laser Line + SB in Up MW Scanning Direction

$K_a = 7 \leftarrow 6, J = 27$



Lamb-Dip Measurements - Completely Resolved Q -Branches

$K_a = 7 \leftarrow 6$ Q branch

$10P(42) + SB$ $922.914293\text{ cm}^{-1}$

($K_a+K_c = J \leftarrow K_a+K_c = J+1$)

J	LDO MHz	LDO cm^{-1}	FTS cm^{-1}	O-C MHz	LDO MHz	O-C MHz	Δ MHz
7	9668.64	923.236804		5.38			
8	9638.97	923.235815		5.21			
9	9604.94	923.234680		5.09			
10	9566.22	923.233388		4.95			
11	9522.58	923.231932		4.87			
12	9473.55	923.230297		4.71			
13	9418.75	923.228469		4.41			
14	9358.03	923.226444		4.19			
15	9290.98	923.224207		4.05			
16	9216.79	923.221732		3.61			
17	9135.46	923.219019	923.219410	3.37			
18	9046.38	923.216048	923.216096	3.18			
19	8949.01	923.212800	923.212837	3.00			
20	8842.65	923.209252	923.209270	2.74			
21	8726.84	923.205389	923.205322	2.47			
22	8601.08	923.201194	923.201094	2.29			
23	8464.56	923.196641	923.196657	2.09			
24	8316.60	923.191705	923.191976	1.84			
25	8156.48	923.186364	923.186381	1.48			
26	7983.64	923.180599	923.180423	1.23			
27	7797.45	923.174388	923.174366	1.18			
28	7596.73	923.167693	923.167702	0.99			
29	7380.82	923.160491	923.160603	0.78			
30	7148.85	923.152753	923.152763	0.55			

($K_a+K_c = J+1 \leftarrow K_a+K_c = J$)

7797.03	1.21	0.42
7596.07	1.02	0.66
7379.76	0.77	1.06
7147.26	0.55	1.59



small Δ splittings have been observed



Ab initio Dipole Derivative for the ν_{11} Band of BDE

- Structure & frequency calculation with Gaussian 03 at B3LYP/6-311++G**
- *Ab initio* frequency calculation gives:

- **Eigenvectors for each normal mode**

(standard orientation, normalized, not orthogonal): $\Phi_n = \{\{\frac{dx}{dQ_n}, \frac{dy}{dQ_n}, \frac{dz}{dQ_n}\}_i\}_{i=1 to 10}$
multiplied by $(m_{rd_n})^{1/2} \Rightarrow PAM$

$(n = 1 \text{ to } 15)$

- **Dipole derivative in z-matrix orientation:**
 $\Rightarrow PAM$

$$\frac{d\mu_g}{dk} = \{\frac{d\mu_g}{dx}, \frac{d\mu_g}{dy}, \frac{d\mu_g}{dz}\}_{i=1 to 10} \quad (g \text{ and } k = x, y, z)$$

- **Dipole derivatives for each normal mode
in PAM system**

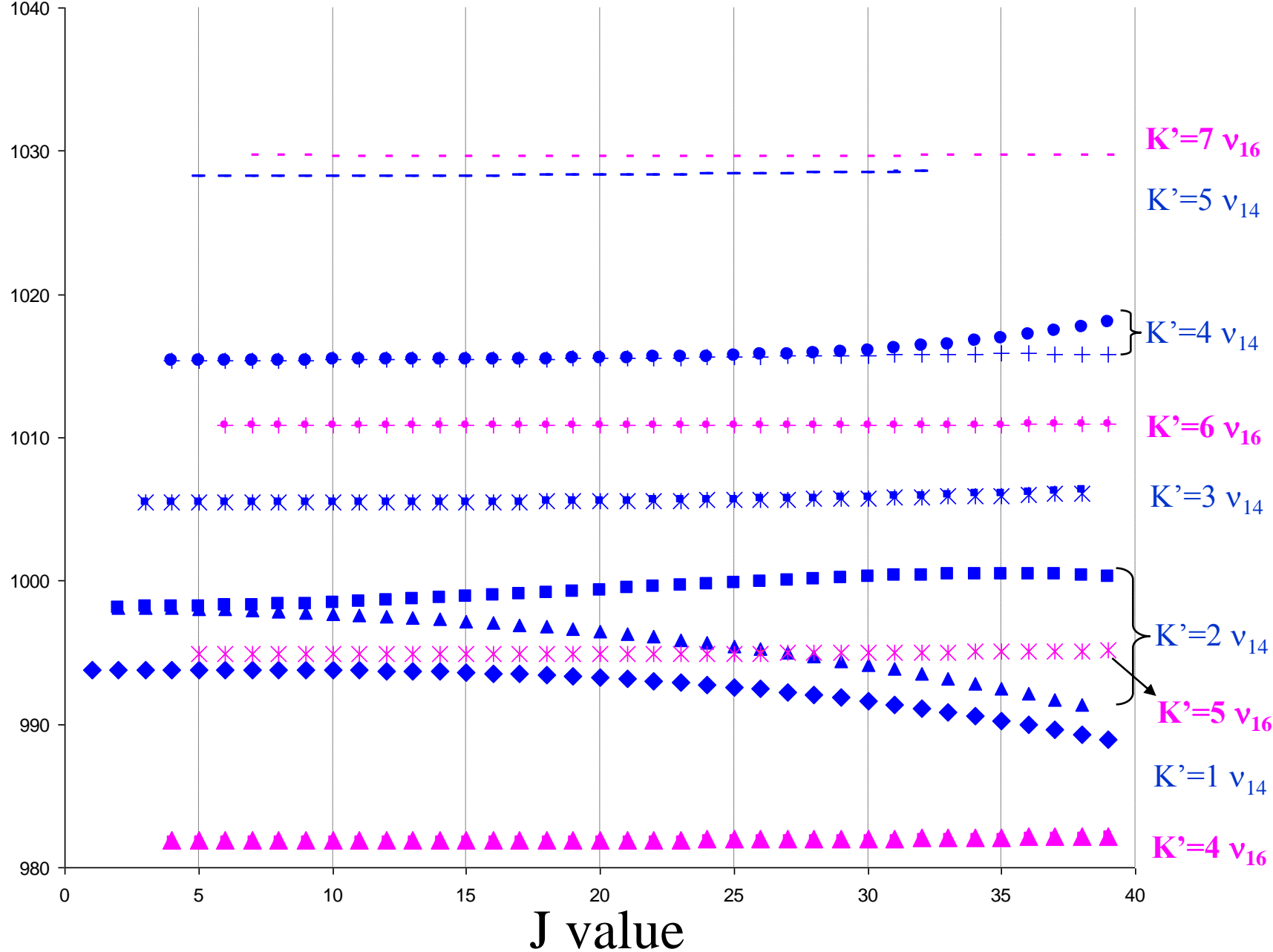
$$\frac{d\mu_g}{dQ_n} = \{\{\frac{d\mu_g}{dx}, \frac{d\mu_g}{dy}, \frac{d\mu_g}{dz}\}_i\} \bullet \{\{\frac{dx}{dQ_n}, \frac{dy}{dQ_n}, \frac{dz}{dQ_n}\}_i\}$$

Ab initio results for 4 Au modes

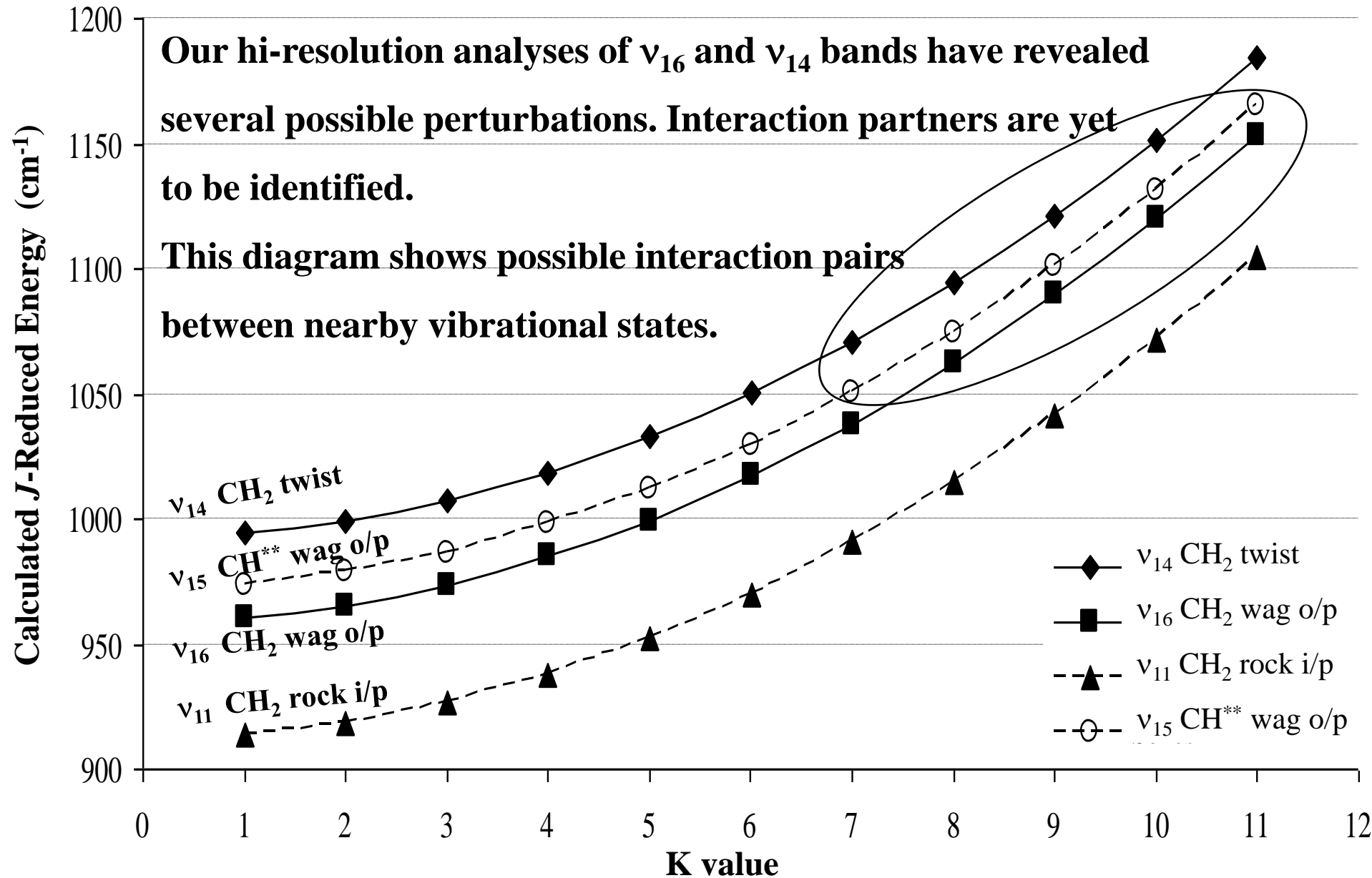
			ν_{11}		
Ab initio output	Harmonic Frequencies (cm ⁻¹)	172.39	534.49	937.36	1051.21
	IR Intensities (km/mol)	0.6983	14.2316	95.8243	36.8438
Our calc	dμ _C /dQ (Debye)	0.02676	-0.1208	-0.3135	-0.1944
	sum(dμ/dQ) ² * cvt	0.6982	14.2313	95.8172	36.8419

(cm⁻¹)

Acrolein J-Reduced Energy Diagram



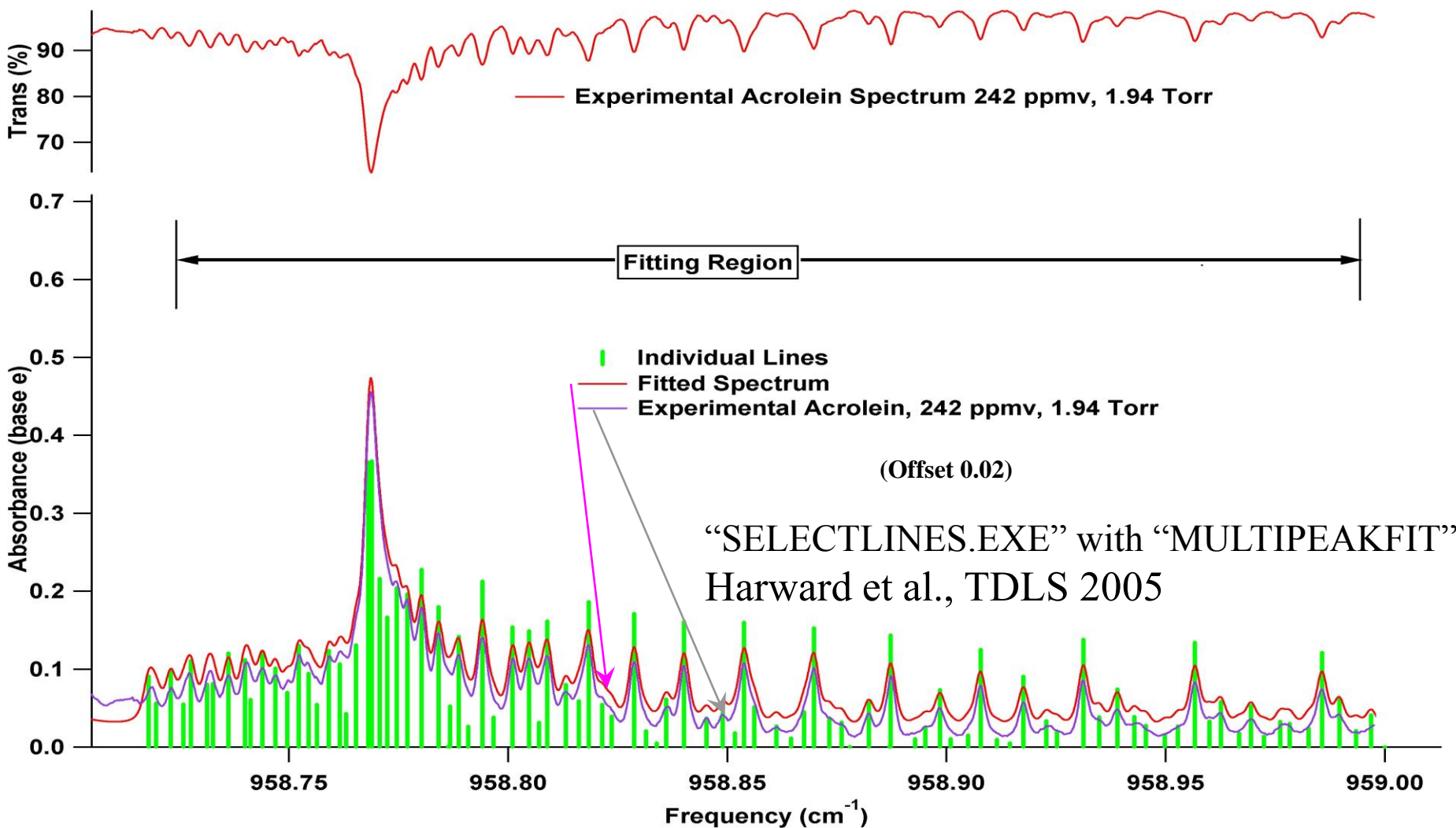
Acrolein J-Reduced Energy Diagram (Calculated)



US-EPA 188 Hazardous Air Pollutants (HAPs)

Acetaldehyde	2-Chloroacetophenone	2,4-Dinitrotoluene	Methoxychlor	1,3-Propane sultone
Acetamide	Chlorobenzene	1,4-Diethyleneoxide	Methyl bromide	beta-Propiolactone
Acetonitrile	Chlorobenzilate	1,2-Diphenylhydrazine	Methyl chloride	Propionaldehyde
Acetophenone	Chloroform	Epichlorohydrin	Methyl chloroform	Propoxur
2-Acetylaminofluorene	Chloromethyl methyl ether	1,2-Epoxybutane	Methyl ethyl ketone	Propylene dichloride
Acrolein	Chloroprene	Ethyl acrylate	Methyl hydrazine	Propylene oxide
Acrylamide	Cresols/Cresylic	Ethyl benzene	Methyl iodide	1,2-Propylenimine
Acrylic acid	o-Cresol	Ethyl carbamate	Methyl isobutyl ketone	Quinoline
Acrylonitrile	m-Cresol	Ethyl chloride	Methyl isocyanate	Quinone
Allyl chloride	p-Cresol	Ethylene dibromide	Methyl methacrylate	Styrene
4-Aminobiphenyl	Cumene	Ethylene dichloride	Methyl tert butyl ether	Styrene oxide
Aniline	2,4-D, salts and esters	Ethylene glycol	4,4-Methylene bis(2-chloroaniline)	2,3,7,8-Tetrachlorodibenzo-p-dioxin
o-Anisidine	DDE	Ethylene imine	Methylene chloride	1,1,2,2-Tetrachloroethane
Asbestos	Diazomethane	Ethylene oxide	Methylene diphenyl diisocyanate	Tetrachloroethylene
Benzene	Dibenzofurans	Ethylene thiourea	4,4-Methylenedianiline	Titanium tetrachloride
Benzidine	1,2-Dibromo-3-chloropropane	Ethyldene dichloride	Naphthalene	Toluene
Benzotrichloride	Dibutylphthalate	Formaldehyde	Nitrobenzene	2,4-Toluene diamine
Benzyl chloride	1,4-Dichlorobenzene(p)	Heptachlor	4-Nitrobiphenyl	2,4-Toluene diisocyanate
Biphenyl	3,3-Dichlorobenzidene	Hexachlorobenzene	4-Nitrophenol	o-Toluidine
Bis(2-ethylhexyl)phthalate	Dichloroethyl ether	Hexachlorobutadiene	2-Nitropropane	Toxaphene
Bis(chloromethyl)ether	1,3-Dichloropropene	Hexachlorocyclopentadiene	N-Nitroso-N-methylurea	1,2,4-Trichlorobenzene
Bromoform	Dichlorvos	Hexachloroethane	N-Nitrosodimethylamine	1,1,2-Trichloroethane
1,3-Butadiene	Diethanolamine	Hexamethylene-1,6-diisocyanate	N-Nitrosomorpholine	Trichloroethylene
Calcium cyanamide	N,N-Diethyl aniline	Hexamethylphosphoramide	Parathion	2,4,5-Trichlorophenol
Caprolactam	Diethyl sulfate	Hexane	Pentachloronitrobenzene	2,4,6-Trichlorophenol
Captan	3,3-Dimethoxybenzidine	Hydrazine	Pentachlorophenol	Triethylamine
Carbaryl	Dimethyl aminoazobenzene	Hydrochloric acid	Phenol	Trifluralin
Carbon disulfide	3,3'-Dimethyl benzidine	Hydrogen fluoride	p-Phenylenediamine	2,2,4-Trimethylpentane
Carbon tetrachloride	Dimethyl carbamoyl chloride	Hydrogen sulfide	Phosgene	Vinyl acetate
Carbonyl sulfide	Dimethyl formamide	Hydroquinone	Phosphine	Vinyl bromide
Catechol	1,1-Dimethyl hydrazine	Isophorone	Phosphorus	Vinyl chloride
Chloramben	Dimethyl phthalate	Lindane (all isomers)	Phthalic anhydride	Vinylidene chloride
Chlordane	Dimethyl sulfate	Maleic anhydride	Polychlorinated biphenyls	Xylenes
Chlorine	4,6-Dinitro-o-cresol, and salts	Methanol		
Chloroacetic acid	2,4-Dinitrophenol			

“Pseudo” line lists from TDL spectra: Acrolein



For better intensity information from the hi-resolution spectra by “scaling” to the low resolution TDL spectra where intensity information is known accurately.

Acrolein Detection Scheme

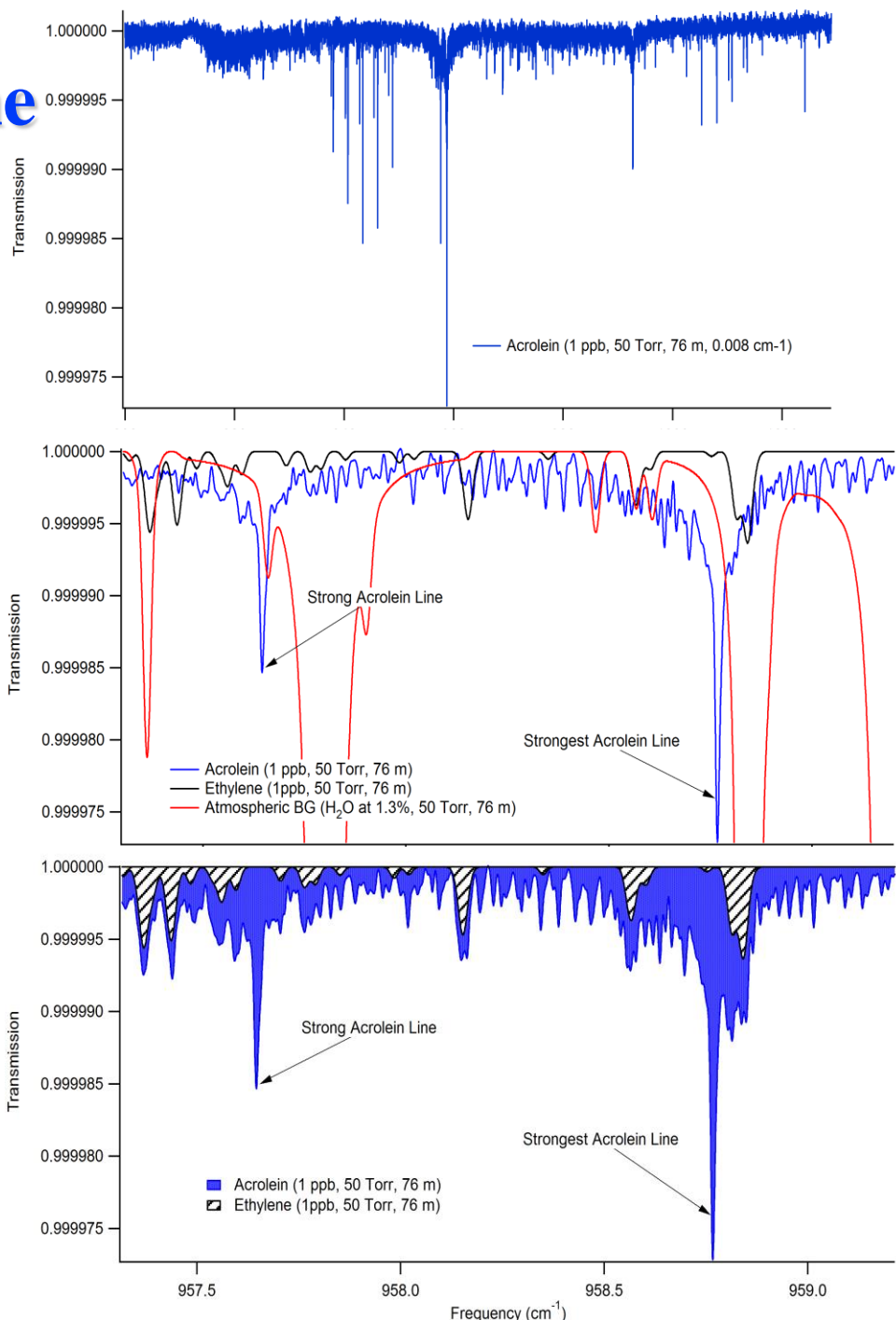
High resolution FTIR Spectrum obtained from NRC (scaled to low TDL od spectra)

Linestrengths from Harward et al. (2005), scaled to 76 m, 1 ppb, 50 Torr
Abs max: 3×10^{-5}

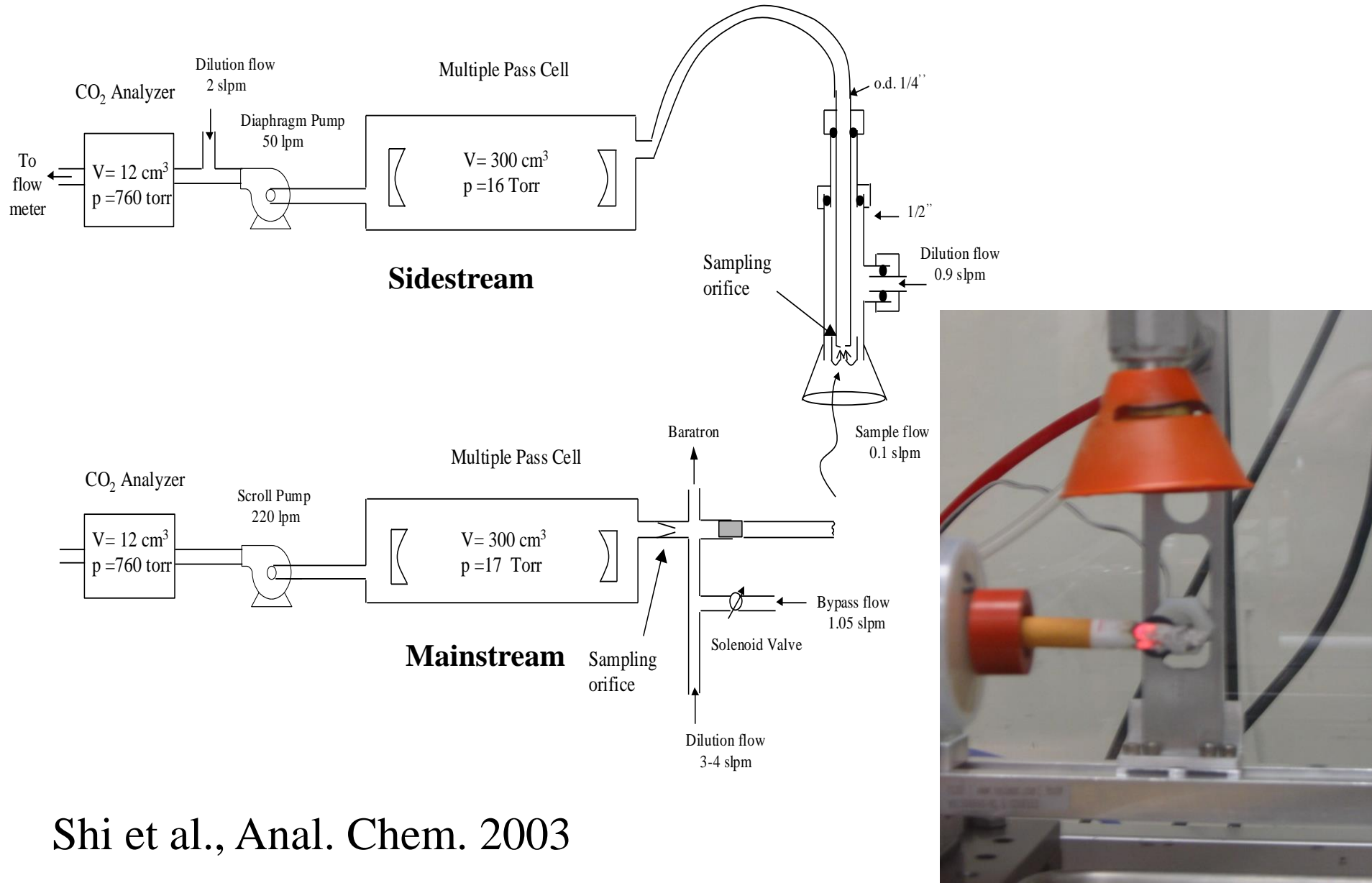
Strongest features at 958 cm^{-1} with atmospheric background $\text{CO}_2, \text{H}_2\text{O}$

Background subtracted spectrum with Ethylene, 1 ppb

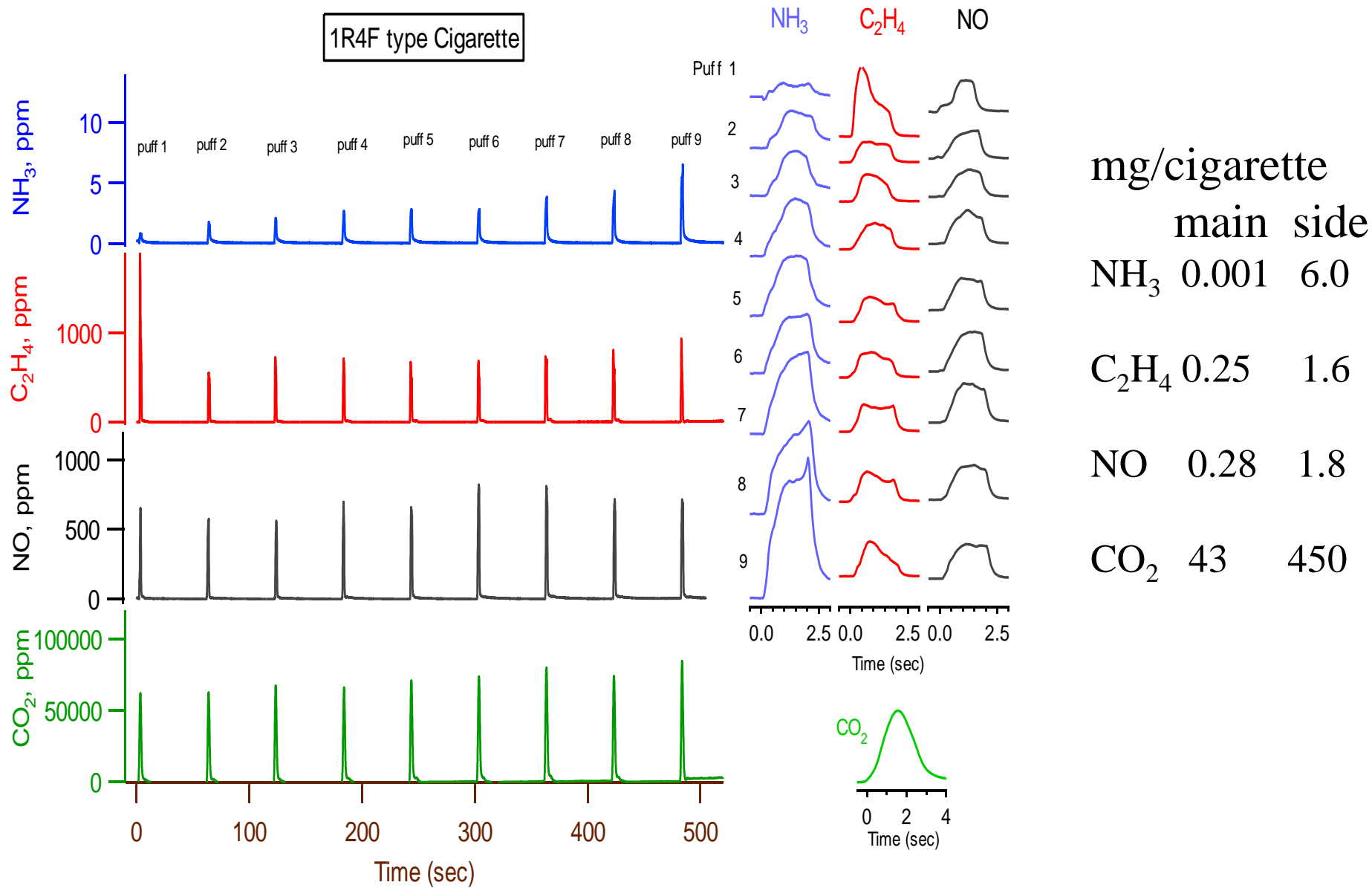
Acrolein Detection limit:
0.4 ppb (2s, 60 s)



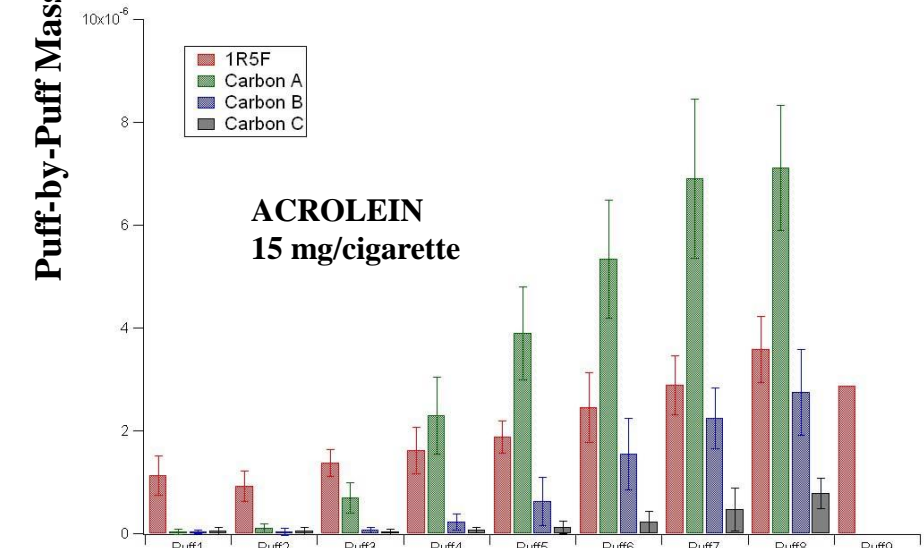
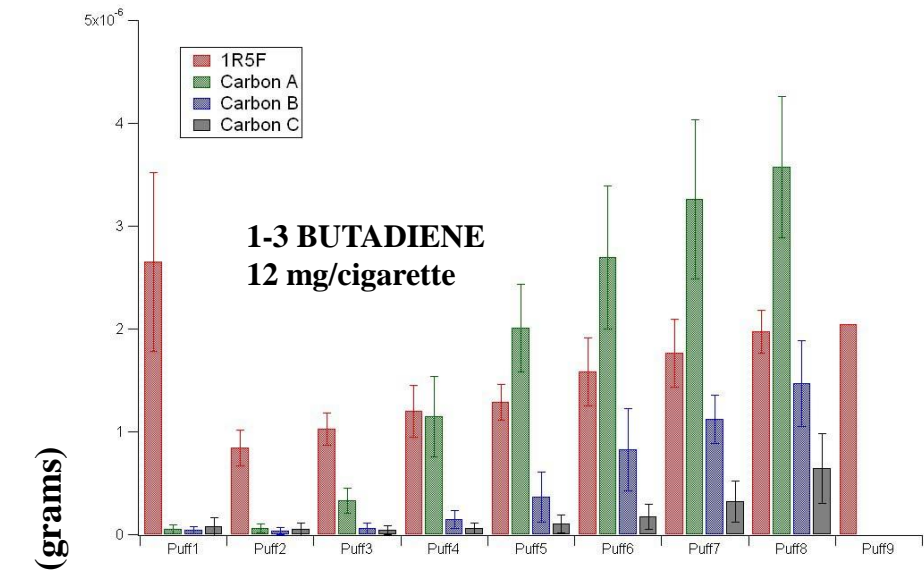
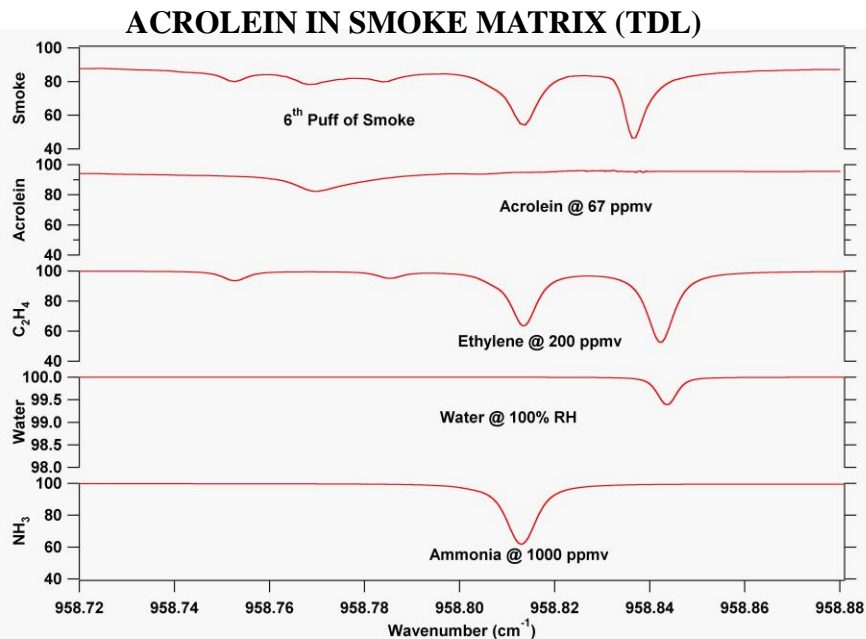
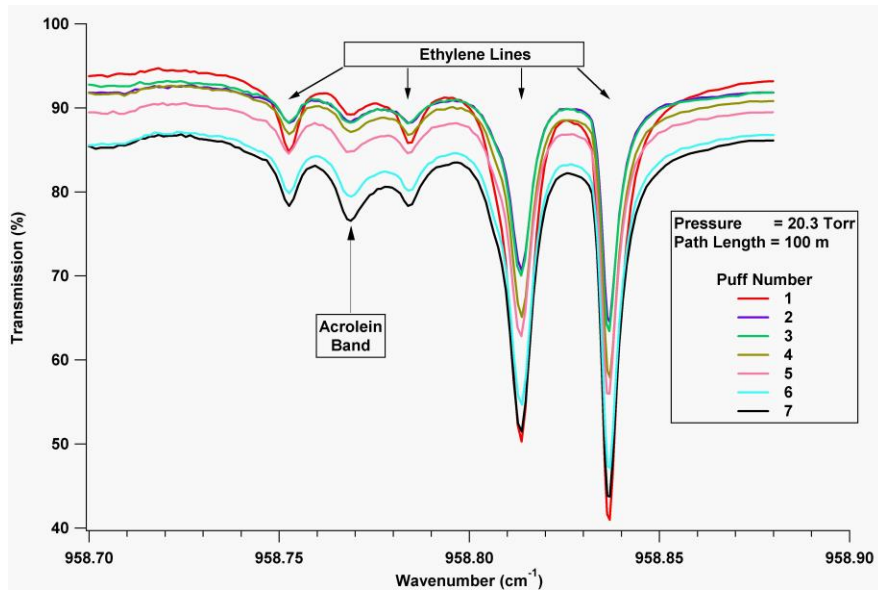
Cigarette Smoke Analysis



Cigarette Smoke Analysis with QCLs



Acrolein Cigarette Smoke (TDL Spectra)



Ref: Harward, Thweatt, Parrish; TDLS 2005